ISET Journal of Earthquake Technology, Paper No. 467, Vol. 43, No. 1-2, March-June 2006, pp. 1-9

SCATTERING OF SEISMIC WAVES FROM A CIRCULAR CAVITY WITH A PARTIALLY DEBONDED LINER

Gui-Lan Yu and Yue-Sheng Wang
School of Civil Engineering and Architecture
Beijing Jiaotong University
Beijing 100044, China

ABSTRACT

The scattering of seismic waves by a circular cavity with a partially debonded liner is studied by using the wave function expansion method and singular integral equation technique. The debonding region is modeled as an arc-shaped interface crack. For simplicity, the interaction between the crack edges is neglected. By expanding the wave fields in both liner and matrix as Fourier-Bessel series, the mixed boundary conditions lead to a set of simultaneous dual series equations, which may be further converted to Hilbert singular integral equations. Dynamic stress intensity factors describing the strength of dynamic interface traction at the ends of the bonding region and the scattering cross section are calculated by solving the singular integral equations numerically. The results show a distinguishing feature, the low frequency resonance, of such a problem.

KEYWORDS: Scattering, Seismic Wave, Interface Debonding, Liner

INTRODUCTION

Scattering of seismic waves from a cavity with a liner is an interesting problem in earthquake engineering and civil engineering and has received considerable attention. The problem is customarily treated on the assumption that the liner is perfectly bonded to the matrix. For instance, Mal et al. (1968) solved the scattering of single objects within an infinite medium or with free surface based on quasi-analytical methods in the frequency domain. However, perfect bonding is not always true in practical cases. For example, partial debonding usually occurs on the interface and may result in catastrophic failure of structures. In the past several decades a large number of valuable results were obtained. The scattering of elastic waves from a partially debonded inclusion was analyzed by Coussy (1984, 1986), Yang and Norris (1992). In the work by Wang and Meguid (1999), the dynamic interaction between a matrix crack and an inclusion subjected to anti-plane incident wave was discussed. The boundary element method (BEM) has also been used to study the scattering of elastic waves by a partially debonded inclusion (Sato and Shindo, 2002). A comprehensive review of BEMs applied to wave propagation phenomena including cracked media is due to Manolis and Beskos (1988), while an extensive study about the interaction of elastic waves with cracks was presented by Zhang and Gross (1998). Wang and Wang (1994a) have analytically studied the scattering of an SH wave by a cavity with a partially debonded liner by using the wave function expansion method and singular integral equation technique. Here, in the present paper, scattering of a P or SV wave is examined by using a similar method. The scattering of a plane wave by a partially debonded rigid or elastic cylindrical inclusion has been analyzed by Wang and Wang (1994b, 1996).

PROBLEM FORMULATION

Consider the problem shown in Figure 1. An elastic circular liner, with inner radius r_1 and outer radius r_0, is partially bonded to the matrix. λ, μ, ρ are, respectively, the Lame's constant, shear modulus and mass density. The subscripts "0" and "1" in this paper correspond to the matrix and liner respectively. The polar coordinate (r-θ) system is used. The debonding region is modeled as an interface crack with non-contacting faces, and is denoted by (a, b). An incident plane wave (P or SV) propagates in the direction of θ_0. The entire motion is harmonic in time with frequency ω, and the term $e^{i\omega t}$ will be omitted throughout the paper. For the present in-plane problem, we use the displacement potentials φ

and ψ (Pao and Mow, 1973). For the incident P-wave, the potential is assumed to be $\varphi_0^{(i)} = Ae^{ik_{L0}r\cos(\theta-\theta_0)}$, and for the SV-wave incidence, $\psi_0^{(i)} = Be^{ik_{T0}r\cos(\theta-\theta_0)}$, where A and B are the amplitudes; $K_L = \omega/c_L$ and $K_T = \omega/c_T$ are the longitudinal wave number and shear wave number with $c_L = \sqrt{(\lambda+2\mu)/\rho}$ and $c_T = \sqrt{\mu/\rho}$.

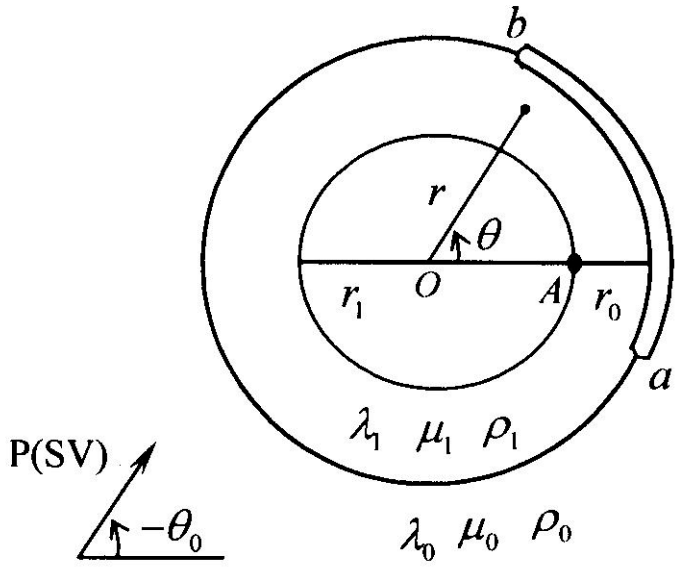

Fig. 1 Scattering of an in-plane wave from a partially bonded liner

The analysis here will focus on the P-wave incidence. The total potentials in the matrix and liner can be decomposed as

$$\left\{\varphi_j, \psi_j\right\} = (1-j)\left\{\varphi_j^{(i)}, 0\right\} + \left\{\varphi_j^{(0)}, \psi_j^{(0)}\right\} + \left\{\varphi_j^{(1)}, \psi_j^{(1)}\right\} \tag{1}$$

where the quantities with superscript "(0)" refer to the scattered fields for a perfectly bonded liner (Pao and Mow, 1973), and those with superscript "(1)" to the additional scattered fields due to debonding. Using the wave function expansion method, we obtain

$$\left\{\varphi_0^{(1)}, \psi_0^{(1)}\right\} = \sum_{m=-\infty}^{\infty} \left\{A_{0m}H_m^{(1)}(K_{L0}r), B_{0m}H_m^{(1)}(K_{T0}r)\right\} e^{-im\theta} \tag{2}$$

$$\left\{\varphi_1^{(1)}, \psi_1^{(1)}\right\} = \sum_{m=-\infty}^{\infty} \left\{[A_{1m}J_m(K_{L1}r) + \overline{A}_{1m}Y_m(K_{L1}r)], [B_{1m}J_m(K_{T1}r) + \overline{B}_{1m}Y_m(K_{T1}r)\right\} e^{-im\theta} \tag{3}$$

where $J_m, Y_m, H_m^{(1)}$ are Bessel functions (Abramowitz and Stegun, 1965). The associated displacement and stress components in the matrix, $\left\{u_0^{(1)}, v_0^{(1)}\right\}$ and $\left\{\sigma_{r0}^{(1)}, \tau_{r\theta 0}^{(1)}\right\}$, are of the same forms as those for the case of cylindrical inclusion (Wang and Wang, 1994b, 1996). The quantities, $\left\{\sigma_{r1}^{(1)}, \tau_{r\theta 1}^{(1)}\right\}$, in the liner are

$$\begin{cases} ru_1^{(1)} = \sum_{m=-\infty}^{\infty} \left[A_{1m}K_{L1}rJ'_m(K_{L1}r) - iB_{1m}mJ_m(K_{T1}r) + \overline{A}_{1m}K_{L1}rY'_m(K_{L1}r) - i\overline{B}_{1m}mY_m(K_{T1}r)\right] e^{-im\theta} \\ rv_1^{(1)} = -\sum_{m=-\infty}^{\infty} \left[B_{1m}K_{T1}rJ'_m(K_{T1}r) + iA_{1m}mJ_m(K_{L1}r) + \overline{B}_{1m}K_{T1}rY'_m(K_{T1}r) + i\overline{A}_{1m}mY_m(K_{L1}r)\right] e^{-im\theta} \end{cases} \tag{4}$$

$$\begin{cases} r^2\sigma_{r1}^{(1)} = \mu_1 \sum_{m=-\infty}^{\infty} \left[A_{1m}T_{11}^{(1)}(K_{L1}r) + B_{1m}T_{12}^{(1)}(K_{T1}r) + \overline{A}_{1m}\overline{T}_{11}^{(1)}(K_{L1}r) + \overline{B}_{1m}\overline{T}_{12}^{(1)}(K_{T1}r)\right] e^{-im\theta} \\ r^2\tau_{r\theta 1}^{(1)} = \mu_1 \sum_{m=-\infty}^{\infty} \left[A_{1m}T_{21}^{(1)}(K_{L1}r) + B_{1m}T_{22}^{(1)}(K_{T1}r) + \overline{A}_{1m}\overline{T}_{21}^{(1)}(K_{L1}r) + \overline{B}_{1m}\overline{T}_{22}^{(1)}(K_{T1}r)\right] e^{-im\theta} \end{cases} \tag{5}$$

with

$$\begin{cases} T_{11}^{(1)}(K_{L0}r) = (2m^2 - K_{T0}^2 r^2)J_m(K_{L0}r) - 2K_{L0}rJ_m'(K_{L0}r) \\ T_{12}^{(1)}(K_{T0}r) = 2im[J_m(K_{T0}r) - K_{T0}rJ_m'(K_{T0}r)] \\ T_{21}^{(1)}(K_{L0}r) = 2im[J_m(K_{L0}r) - K_{L0}rJ_m'(K_{L0}r)] \\ T_{22}^{(1)}(K_{T0}r) = -(2m^2 - K_{T0}^2 r^2)J_m(K_{T0}r) + 2K_{T0}rJ_m'(K_{T0}r) \end{cases} \tag{6}$$

Here, $\overline{T}_{ij}^{(1)}$ is the same as $T_{ij}^{(1)}$, with J_m replaced by Y_m. That the total tractions vanish on the inner surface of the liner, i.e. $\sigma_{r1}^{(1)}(r_1,\theta) = \tau_{r\theta 1}^{(1)}(r_1,\theta) = 0$, yields

$$\begin{cases} \delta\overline{A}_{1m} = X_1 A_{1m} + X_2 B_{1m} \\ \delta\overline{B}_{1m} = X_3 A_{1m} + X_4 B_{1m} \end{cases} \tag{7}$$

where $\delta = \overline{T}_{11}^{(1)}(K_{L1}r_1)\overline{T}_{22}^{(1)}(K_{T1}r_1) - \overline{T}_{21}^{(1)}(K_{L1}r_1)\overline{T}_{12}^{(1)}(K_{T1}r_1)$, $X_i\,(i = 1,2,3,4)$ can be found in the Appendix.

Substitution of (7) into (4) and (5) gives

$$\begin{cases} ru_1^{(1)}(r,\theta) = \sum_{m=-\infty}^{\infty}\left[A_{1m}K_{L1}r\tilde{Z}_{1m}(r) - iB_{1m}mZ_{1m}(r)\right]e^{-im\theta} \\ rv_1^{(1)}(r,\theta) = -\sum_{m=-\infty}^{\infty}\left[B_{1m}K_{T1}r\tilde{Z}_{2m}(r) + iA_{1m}mZ_{2m}(r)\right]e^{-im\theta} \end{cases} \tag{8}$$

$$\begin{cases} r^2\sigma_{r1}^{(1)}(r,\theta) = \mu_0\sum_{m=-\infty}^{\infty}\left[A_{1m}S_{11}^{(1)}(r) + B_{1m}S_{12}^{(1)}(r)\right]e^{-im\theta} \\ r^2\tau_{r\theta 1}^{(1)}(r,\theta) = \mu_0\sum_{m=-\infty}^{\infty}\left[A_{1m}S_{21}^{(1)}(r) + B_{1m}S_{22}^{(1)}(r)\right]e^{-im\theta} \end{cases} \tag{9}$$

where Z_{im}, $\tilde{Z}_{im}$, $S_{ij}^{(1)}$ $(i, j = 1, 2)$ are as given in the Appendix.

The mixed boundary conditions at the interface $r = r_0$ can be written as

$$\begin{cases} u_0^{(1)}(r_0,\theta) - u_1^{(1)}(r_0,\theta) = \Delta u(\theta), \quad v_0^{(1)}(r_0,\theta) - v_1^{(1)}(r_0,\theta) = \Delta v(\theta) \\ \sigma_{r0}^{(1)}(r_0,\theta) = \sigma_{r1}^{(1)}(r_0,\theta), \quad \tau_{r\theta 0}^{(1)}(r_0,\theta) = \tau_{r\theta 1}^{(1)}(r_0,\theta) \\ \sigma_{r0}^{(1)}(r_0,\theta) = -\sigma_{r1}^{(0)}(r_0,\theta) = -[\sigma_{r0}^{(i)}(r_0,\theta) + \sigma_{r0}^{(0)}(r_0,\theta)]; \quad \theta \in (a,b) \\ \tau_{r\theta 0}^{(1)}(r_0,\theta) = -\tau_{r\theta 1}^{(0)}(r_0,\theta) = -[\tau_{r\theta 0}^{(i)}(r_0,\theta) + \tau_{r\theta 0}^{(0)}(r_0,\theta)]; \quad \theta \in (a,b) \end{cases} \tag{10}$$

Here, Δu and Δv are crack opening displacements which are zero beyond the crack.

SINGULAR INTEGRAL EQUATIONS

We expand $\Delta u(\theta)$ and $\Delta v(\theta)$ in the form of Fourier series:

$$\Delta u(\theta) = \sum_{m=-\infty}^{\infty}\Delta\overline{u}_m e^{-im\theta}, \quad \Delta v(\theta) = \sum_{m=-\infty}^{\infty}\Delta\overline{v}_m e^{-im\theta} \tag{11}$$

with

$$\Delta\overline{u}_m = \frac{1}{2\pi}\int_a^b \Delta\overline{u}(\varsigma)e^{im\varsigma}d\varsigma, \quad \Delta\overline{v}_m = \frac{1}{2\pi}\int_a^b \Delta\overline{v}(\varsigma)e^{im\varsigma}d\varsigma \tag{12}$$

Then A_{jm} and B_{jm} can be expressed in terms of $\Delta\overline{u}_m$ and $\Delta\overline{v}_m$ by considering Equations (8) and the first two of Equations (10). Substituting the results into (9) and taking into account the last two of Equations (10), we obtain

$$\begin{cases} \mu_0 \sum_{m=-\infty}^{m=\infty} [N_m^{(11)} \Delta\overline{u}_m + N_m^{(12)} \Delta\overline{v}_m] e^{-im\theta} = -\sigma_{r1}^{(0)}(r_0, \theta) \\ \mu_0 \sum_{m=-\infty}^{m=\infty} [N_m^{(21)} \Delta\overline{u}_m + N_m^{(22)} \Delta\overline{v}_m] e^{-im\theta} = -\tau_{r\theta 1}^{(0)}(r_0, \theta) \end{cases} ; \quad \theta \in (a,b) \tag{13}$$

where $N_m^{(ij)}$ is expressed as

$$\begin{cases} N_m^{(j1)} = r_0^{-1} D_m^{-1} [T_{j1}^{(0)}(K_{L0} r_0) U_{0m}^{(1)} + T_{j2}^{(0)}(K_{T0} r_0) U_{0m}^{(2)}] \\ N_m^{(j2)} = r_0^{-1} D_m^{-1} [T_{j1}^{(0)}(K_{L0} r_0) V_{0m}^{(1)} + T_{j2}^{(0)}(K_{T0} r_0) V_{0m}^{(2)}] \end{cases} \tag{14}$$

with
$$D_m = \begin{vmatrix} T_{11}^{(0)}(K_{L0} r_0) & T_{12}^{(0)}(K_{T0} r_0) & -S_{11}^{(1)}(r_0) & -S_{12}^{(1)}(r_0) \\ T_{21}^{(0)}(K_{L0} r_0) & T_{22}^{(0)}(K_{T0} r_0) & -S_{21}^{(1)}(r_0) & -S_{22}^{(1)}(r_0) \\ K_{L0} r_0 H_m^{(1)\prime}(K_{L0} r_0) & -imH_m^{(1)}(K_{T0} r_0) & -K_{L1} r_0 \tilde{Z}_{1m}(r_0) & imZ_{1m}(r_0) \\ -imH_m^{(1)}(K_{L0} r_0) & -K_{T0} r_0 H_m^{(1)\prime}(K_{T0} r_0) & imZ_{2m}(r_0) & K_{T1} r_0 \tilde{Z}_{2m}(r_0) \end{vmatrix} \tag{15}$$

and
$$U_{jm}^{(k)} = \overline{D}_{3,k+2j}, \quad V_{jm}^{(k)} = \overline{D}_{4,k+2j}; \quad j = 0,1 \quad k = 1,2 \tag{16}$$

Here, $\overline{D}_{i,j}$ denotes the algebraic complement of the element of the *i*th row and *j*th column of D_m.

Outside the debonding region, we have

$$\sum_{m=-\infty}^{m=\infty} \Delta\overline{u}_m e^{-im\theta} = 0, \quad \sum_{m=-\infty}^{m=\infty} \Delta\overline{v}_m e^{-im\theta} = 0; \quad \theta \notin (a,b) \tag{17}$$

Equations (13) and (17) are indeed a set of dual series equations. Introducing the following crack dislocation density functions (Wang and Wang, 1994b, 1996),

$$\varphi(\theta) = \frac{1}{r_0} \frac{\partial}{\partial\theta}(\Delta u), \quad \psi(\theta) = \frac{1}{r_0} \frac{\partial}{\partial\theta}(\Delta v) \tag{18}$$

Equations (13) reduce to

$$\begin{cases} \frac{i}{2\pi} \int_a^b \sum_{m=-\infty}^{\infty} [M_m^{(11)} \varphi(\varsigma) + M_m^{(12)} \psi(\varsigma)] e^{im(\zeta-\theta)} d\varsigma = -\sigma_{r1}^{(0)}(r_0, \theta) \\ \frac{i}{2\pi} \int_a^b \sum_{m=-\infty}^{\infty} [M_m^{(21)} \varphi(\varsigma) + M_m^{(22)} \psi(\varsigma)] e^{im(\zeta-\theta)} d\varsigma = -\tau_{r\theta 1}^{(0)}(r_0, \theta) \end{cases} ; \quad \theta \in (a,b) \tag{19}$$

with $M_0^{(st)} = i\mu_0 r_0 N_0^{(st)}[\varsigma - (a+b)/2]$ and $M_m^{(st)} = \mu_0 r_0 N_m^{(st)} / m; \; s,t = 1,2$. Considering the asymptotic behavior of Bessel functions, $J_m, Y_m, H_m^{(1)}$, as $m \to \pm\infty$ (Abramowitz and Stegun, 1965), we have

$$M_m^{(11)}, \; M_m^{(22)} \sim \beta - \alpha / m + O(m^{-2}); \; m \to \pm\infty \tag{20}$$

where α and β are the two important parameters defined by Dundurs (1969) to characterize the bimaterial system. With the relations given in (20), we can transform Equations (19), as in Wang and Wang (1994b, 1996), into a set of singular integral equations of the second type:

$$\begin{cases} -a\psi(\theta) - \frac{\beta}{2\pi} \int_a^b \varphi(\varsigma) \cot\left(\frac{\varsigma - \theta}{2}\right) d\varsigma + \int_a^b [\varphi(\varsigma) P_{11} + \psi(\varsigma) P_{12}] d\varsigma = -\sigma_{r1}^{(0)}(r_0, \theta) \\ a\psi(\theta) - \frac{\beta}{2\pi} \int_a^b \psi(\varsigma) \cot\left(\frac{\varsigma - \theta}{2}\right) d\varsigma + \int_a^b [\varphi(\varsigma) P_{21} + \psi(\varsigma) P_{22}] d\varsigma = -\tau_{r\theta 1}^{(0)}(r_0, \theta) \end{cases} ; \quad \theta \in (a,b) \tag{21}$$

with

$$P_{st}(\varsigma,\theta) =$$

$$\begin{cases} \dfrac{i}{2\pi}\left\{\left[M_0^{st} + 2i\sum\limits_{m=-\infty}^{\infty}\left(M_m^{st} - \beta\,\mathrm{sgn}(m) + \dfrac{\alpha}{m}\right)\sin m(\varsigma-\theta) - i\alpha\left[\pi\,\mathrm{sgn}(\varsigma-\theta) - (\varsigma-\theta)\right]\right]\right\}; & s = t \\ (-1)^t\dfrac{i}{2\pi}\left\{\left[-i\alpha + 2\sum\limits_{m=-\infty}^{\infty}\left(M_m^{st} + (-1)^s i\left(\alpha - \dfrac{\beta}{m}\right)\right)\cos m(\varsigma-\theta) + 2i\beta\ln\left|2\sin\left(\dfrac{\varsigma-\theta}{2}\right)\right|\right]\right\}; & s \neq t \end{cases} \tag{22}$$

It follows from Equations (17) that

$$\int_a^b \left\{\phi(\varsigma),\psi(\varsigma)\right\} d\varsigma = 0 \tag{23}$$

Introducing substitutions $(\theta,\varsigma) = c(\xi,\eta) + d$ with $c = (b-a)/2,\ d = (b+a)/2$ and

$$\begin{Bmatrix} f(\eta) \\ g(\eta) \end{Bmatrix} = [R]^{-1}\begin{Bmatrix} \varphi(c\eta+d) \\ \psi(c\eta+d) \end{Bmatrix},\ \bar{P}_{st}(\eta,\xi) = \frac{i}{\beta}P_{st}(c\eta+d, c\xi+d) \tag{24}$$

with $[R] = \begin{bmatrix} i & -i \\ 1 & 1 \end{bmatrix}$, Equations (21) can be rewritten as a set of standard Cauchy singular integral equations:

$$\begin{bmatrix} -\gamma & 0 \\ 0 & \gamma \end{bmatrix}\begin{Bmatrix} f(\xi) \\ g(\xi) \end{Bmatrix} + \frac{1}{\pi i}\int_{-1}^{1}\begin{bmatrix} 1 & 0 \\ 0 & 1 \end{bmatrix}\begin{Bmatrix} f(\eta) \\ g(\eta) \end{Bmatrix}\frac{d\eta}{\eta-\xi} + c\int_{-1}^{1}\begin{bmatrix} Q_{11} & Q_{12} \\ Q_{21} & Q_{22} \end{bmatrix}\begin{Bmatrix} f(\eta) \\ g(\eta) \end{Bmatrix} d\eta = \begin{Bmatrix} \sigma(\xi) \\ \tau(\xi) \end{Bmatrix};\ |\xi| < 1 \tag{25}$$

Here, we have $\gamma = \alpha/\beta$, and

$$\begin{bmatrix} Q_{11} & Q_{12} \\ Q_{21} & Q_{22} \end{bmatrix} = [R]^{-1}\begin{bmatrix} P_{11} & P_{12} \\ P_{21} & P_{22} \end{bmatrix}[R] + \frac{[I]}{2\pi i}\left[\cot\frac{c(\eta-\xi)}{2} - \frac{2}{c(\eta-\xi)}\right],\ \begin{Bmatrix} \sigma(\xi) \\ \tau(\xi) \end{Bmatrix} = -\frac{[R]^{-1}}{i\beta}\begin{Bmatrix} \sigma_{r1}^{(0)}(c\xi+d) \\ \tau_{r\theta 1}^{(0)}(c\xi+d) \end{Bmatrix} \tag{26}$$

The fundamental solution matrix of Equations (25) is

$$\begin{Bmatrix} W_f(\xi) \\ W_g(\xi) \end{Bmatrix} = \begin{Bmatrix} (1-\xi)^{\bar{\alpha}}(1+\xi)^{\bar{\beta}} \\ (1-\xi)^{\bar{\beta}}(1+\xi)^{\bar{\alpha}} \end{Bmatrix}\ \text{with}\ \begin{Bmatrix} \bar{\alpha} \\ \bar{\beta} \end{Bmatrix} = \begin{Bmatrix} -1/2 - i\lambda \\ -1/2 + i\lambda \end{Bmatrix},\ \lambda = \frac{1}{2\pi}\ln\left(\frac{1+\gamma}{1-\lambda}\right) \tag{27}$$

Then the solution of Equations (25) can be expressed as a series of Jacobi polynomials:

$$\begin{Bmatrix} f(\xi) \\ g(\xi) \end{Bmatrix} = \sum_{j=1}^{\infty}\begin{bmatrix} W_f(\xi) & 0 \\ 0 & W_g(\xi) \end{bmatrix}\begin{Bmatrix} \tilde{A}_j P_j^{(\bar{\alpha},\bar{\beta})}(\xi) \\ \tilde{B}_j P_j^{(\bar{\beta},\bar{\alpha})}(\xi) \end{Bmatrix} \tag{28}$$

which, when substituted into (25), yields an infinite system of linear algebraic equations. Solving these equations by truncating the infinite series to $j = N$, where N is big enough to ensure the convergence, we can obtain the unknown coefficients $\tilde{A}_j$ and $\tilde{B}_j$. For details, reference may be made to Wang and Wang (1996).

NUMERICAL RESULTS AND DISCUSSIONS

Debonding of the interface under stress waves depends on the interface traction near the ends of the crack, which may be described by the dynamic stress intensity factors (DSIFs). Here we follow the method in Wang and Wang (1994b, 1996) to calculate the DSIFs. We define the following equivalent stress components:

$$\left\{\sigma_r^{(e)}, \tau_{r\theta}^{(e)}\right\}^T = -i\beta^{-1}[R]^{-1}\left\{\sigma_r, \tau_{r\theta}\right\}^T \tag{29}$$

They have following asymptotic behavior at the crack tips (e.g., at $\theta \to b^+$, or equivalently at $\xi \to 1^+$):

$$\begin{Bmatrix}\sigma_r^{(e)}(r_0,\xi)\\ \tau_{r\theta}^{(e)}(r_0,\xi)\end{Bmatrix}\approx\begin{Bmatrix}K_{\mathrm{I}b}^{(e)}(r_0c)^{-1/2}(\xi-1)^{\bar{\alpha}}(\xi+1)^{\bar{\beta}}\\ K_{\mathrm{II}b}^{(e)}(r_0c)^{-1/2}(\xi-1)^{\bar{\beta}}(\xi+1)^{\bar{\alpha}}\end{Bmatrix};\quad \xi\to+1 \tag{30}$$

where the equivalent DSIFs, $K_{\mathrm{I}b}^{(e)}$ and $K_{\mathrm{II}b}^{(e)}$, can be computed by (Wang and Wang, 1994b, 1996)

$$\left\{K_{\mathrm{I}b}^{(e)},\quad K_{\mathrm{II}b}^{(e)}\right\}i\sqrt{(1-\gamma^2)r_0c}\sum_{j=1}^{\infty}\left\{\tilde{A}_jP_j^{(\bar{\alpha},\bar{\beta})}(1),\quad \tilde{B}_jP_j^{(\bar{\beta},\bar{\alpha})}(1)\right\} \tag{31}$$

The real DSIFs are given by

$$\left\{K_{\mathrm{I}b},K_{\mathrm{II}b}\right\}^{\mathrm{T}}=i\beta[R]\left\{K_{\mathrm{I}b}^{(e)},K_{\mathrm{II}b}^{(e)}\right\}^{\mathrm{T}} \tag{32}$$

The far-field solution is also of importance in practical cases. By using the asymptotic behavior of Bessel functions at $r\to\infty$ (Abramowitz and Stegun, 1965), the scattered far-field displacements can be expressed as

$$\begin{cases}u_0^{(0)}(r,\theta)+u_0^{(1)}(r,\theta)\approx iK_{L0}\sqrt{\dfrac{8\pi}{K_{L0}r}}e^{i(K_{L0}r-\pi/4)}[F_r^{(0)}(\theta,\theta_0)+F_r^{(1)}(\theta,\theta_0)]\\ v_0^{(0)}(r,\theta)+v_0^{(1)}(r,\theta)\approx iK_{T0}\sqrt{\dfrac{8\pi}{K_{T0}r}}e^{i(K_{T0}r-\pi/4)}[F_\theta^{(0)}(\theta,\theta_0)+F_\theta^{(1)}(\theta,\theta_0)]\end{cases};\quad r\to\infty \tag{33}$$

where $F^{(0)}$ is the scattered far-field pattern for a perfectly bonded liner (Pao and Mow, 1973); and $F^{(1)}$ is that due to debonding, which is given by

$$\left\{F_r^{(1)}(\theta,\theta_0),F_\theta^{(1)}(\theta,\theta_0)\right\}=(2\pi)^{-1}\sum_{m=-\infty}^{\infty}(-i)^m\left\{A_m,B_m\right\}e^{-im\theta} \tag{34}$$

With the above results, we can calculate the total scattering cross-section (SCS). This is defined as $\sigma(\omega)=\left\langle P^S\right\rangle/\left\langle\dot{e}_0\right\rangle$ where $\left\langle\dot{e}_0\right\rangle$ is the time-average of the incident flux and $\left\langle P^S\right\rangle$ is the total scattered energy flux given by (Pao and Mow, 1973)

$$\left\langle P^S\right\rangle=\frac{\omega}{2}\mathrm{Im}\int_S\left[\left(u_0^{(0)}+u_0^{(1)}\right)^*\left(\sigma_{r0}^{(0)}+\sigma_{r0}^{(1)}\right)+\left(v_0^{(0)}+v_0^{(1)}\right)^*\left(\tau_{r\theta0}^{(0)}+\tau_{r\theta0}^{(1)}\right)\right]ds \tag{35}$$

with the asterisk representing conjugation. Choosing *S* to be a unit length cylindrical surface with infinitely large radius, we then have

$$\left\langle P^S\right\rangle=4\pi\omega\mu_0K_{T0}^2\int_{-\pi}^{\pi}\left[\left|F_r^{(0)}+F_r^{(1)}\right|^2+\left|F_\theta^{(0)}+F_\theta^{(1)}\right|^2\right]d\theta \tag{36}$$

The DSIFs and SCS have been computed for different sizes of the debond and for different thicknesses of the liner. We take $\mu_1:\mu_0=20:1$, $\rho_1:\rho_0=5:1$, and Poisson's ratio $\nu_1=\nu_0=0.333$. The incident P-wave propagates along the *x*-axis (i.e., $\theta_0=0^{\mathrm{o}}$). The debond is supposed to be at the shadow side and symmetric about the *x*-axis, that is $a+b=0$. In solving Equation (28) numerically, we should appropriately choose *N* not only to ensure an adequate level of accuracy, but also to avoid wastage of time in computations. To this end, we have computed the normalized DSIFs, SCS and displacement of point A (see Figure 1) at the inner surface of the liner with different values of *N* and listed the results in Table 1. It can be seen that *N* > 14 may give good accuracy. Therefore we choose *N* = 16 in the following calculations.

The results are demonstrated in Figures 2 and 3 where α is the semi-angular width of the debond and $\tau=\mu_0K_{L0}^2A$. In Figures 2(a) and 3(a), the solid lines correspond to K_{I}, and the dashed lines to K_{II}. Figure 2 shows the influence of the debond size for $r_1/r_0=0.5$. A "low-frequency resonance" phenomenon is observed in DSIFs, SCS, and displacement of point A at the inner surface of the liner. The resonance is more pronounced and appears at a low frequency for a large debond. This is understood by considering the fact that, with the value of r_1/r_0 being given (i.e., the mass of the system being fixed), an increase in the debond size α leads to a decrease in the rigidity of the system and, thus, results in a lower

resonant frequency. This phenomenon has been discussed extensively by Wang and Wang (1994a, 1994b, 1996). Figure 3 shows the influence of the thickness of the liner for $\alpha = 150^{o}$. It is seen that the resonant frequency varies with the thickness of the liner. The resonance appears at a low frequency for a small ratio r_1 / r_0. Figures 3(a) and 3(b) also show that the low-frequency resonance is more pronounced for a thicker liner. This implies that a thicker liner may fail more easily than a thinner one due to dynamic effects. The physical interpretation of this phenomenon is that, for a fixed value of the debond size α (i.e., for the fixed rigidity of the system), a decrease in the ratio r_1 / r_0 leads to an increase in the mass of the system and therefore results in a lower resonant frequency. However, the thickness of the liner has little influence on the resonant peak of the displacement as shown in Figure 3(c).

Table 1: Normalized DSIFs, SCS and Displacement of Point A with Different Values of *N* for $K_{T0}r_0$ = 0.5, r_1/r_0 = 0.5, and α = 150°

N	**2**	**4**	**6**	**8**	**10**	**12**	**14**	**16**	**18**	**20**
$K_{\mathrm{I}}/\tau\sqrt{\mathrm{r}_0}$	0.9653	1.4074	3.1840	5.0948	4.1035	4.0827	3.9755	3.9313	3.9677	3.9720
$K_{\mathrm{II}}/\tau\sqrt{\mathrm{r}_0}$	0.1572	1.6365	6.0761	3.4328	2.8332	2.8309	2.7651	2.8481	2.8647	2.8577
σ/r_0	1.9243	3.3562	8.6387	8.1502	7.7972	7.8077	7.8084	7.8172	7.8132	7.8095
$u/K_{L0}A$	1.2368	1.6645	2.6572	2.4219	2.3238	2.3254	2.3274	2.3293	2.3288	2.3282

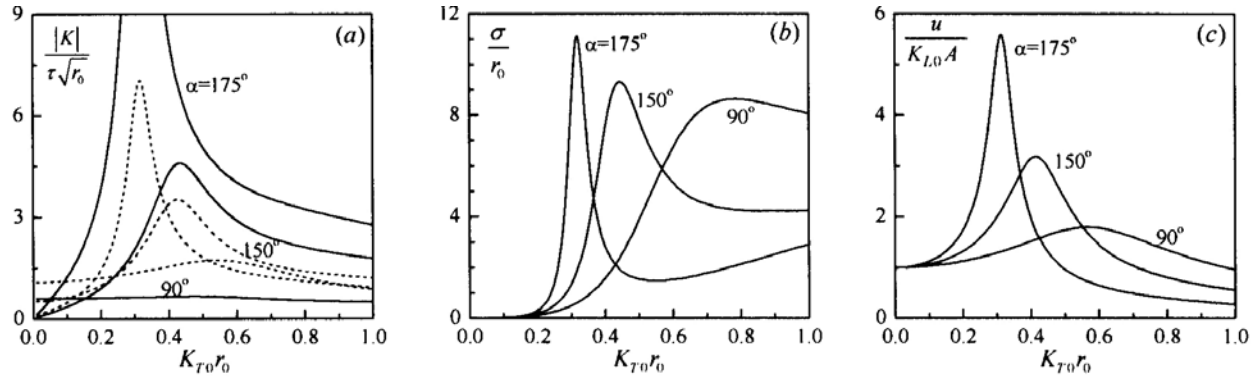

Fig. 2 DSIF, SCS and displacement of point A at the inner surface of the liner for different sizes of the debond with r_1/r_0 = 0.5

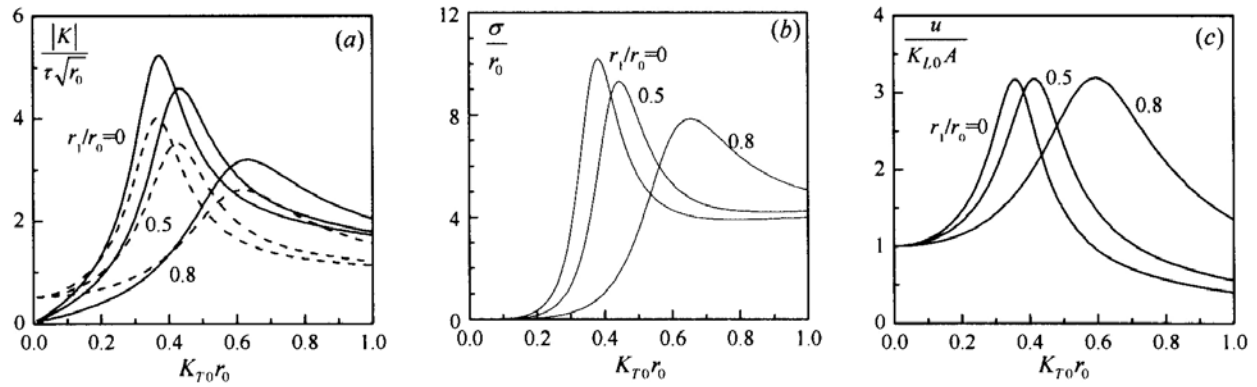

Fig. 3 DSIF, SCS and displacement of point A at the inner surface of the liner for different thicknesses of the liner with α = 150°

These results can be verified by the fact that the present results for $r_1 / r_0 \to 0$ are the same as those obtained by Wang and Wang (1996). Furthermore, the results of a perfectly bonded liner (Pao and Mow, 1973) may be recovered from the present analysis by taking the limit of $\alpha \to 0$.

ACKNOWLEDGEMENTS

This work was supported by the China National Science Foundation under Grant No. 10372001. The second author is also grateful to the support of the National Science Fund for Distinguished Young Scholars under Grant No. 10025211.

APPENDIX

X_i $(i = 1,2,3,4)$ in Equations (7) and $Z_{im}, \tilde{Z}_{im}, S_{ij}^{(1)}$ $(i, j = 1,2)$ in Equations (8) and (9) are as follows:

$$\begin{aligned} X_1 &= T_{21}^{(1)}(K_{L1}r_1)\bar{T}_{12}^{(1)}(K_{T1}r_1) - T_{11}^{(1)}(K_{L1}r_1)\bar{T}_{22}^{(1)}(K_{T1}r_1) \\ X_2 &= T_{22}^{(1)}(K_{L1}r_1)\bar{T}_{12}^{(1)}(K_{T1}r_1) - T_{12}^{(1)}(K_{L1}r_1)\bar{T}_{22}^{(1)}(K_{T1}r_1) \\ X_3 &= T_{11}^{(1)}(K_{L1}r_1)\bar{T}_{21}^{(1)}(K_{L1}r_1) - T_{21}^{(1)}(K_{L1}r_1)\bar{T}_{11}^{(1)}(K_{L1}r_1) \\ X_4 &= T_{12}^{(1)}(K_{T1}r_1)\bar{T}_{21}^{(1)}(K_{L1}r_1) - T_{22}^{(1)}(K_{T1}r_1)\bar{T}_{1\,1}^{(1)}(K_{L1}r_1) \end{aligned} \tag{A.1}$$

$$Z_{1m}(r) = J_m(K_{T1}r) + \frac{1}{\delta}\left[Y_m(K_{T1}r)X_4 - \frac{K_{L1}rY_m'(K_{L1}r)}{im} X_2 \right] \tag{A.2}$$

$$Z_{2m}(r) = J_m(K_{L1}r) + \frac{1}{\delta}\left[Y_m(K_{L1}r)X_1 + \frac{K_{T1}rY_m'(K_{T1}r)}{im} X_3 \right] \tag{A.3}$$

$$\tilde{Z}_{1m}(r) = J_m'(K_{L1}r) + \frac{1}{\delta}\left[Y_m'(K_{L1}r)X_1 - \frac{imY_m(K_{T1}r)}{K_{L1}r} X_3 \right] \tag{A.4}$$

$$\tilde{Z}_{2m}(r) = J_m'(K_{T1}r) + \frac{1}{\delta}\left[Y_m'(K_{T1}r)X_4 + \frac{imY_m(K_{L1}r)}{K_{T1}r} X_2 \right] \tag{A.5}$$

$$S_{i1}^{(1)}(r) = T_{i1}^{(1)}(K_{L1}r) + \frac{1}{\delta}\left[\bar{T}_{i1}^{(1)}(K_{L1}r)X_1 + \bar{T}_{i2}^{(1)}(K_{T1}r)X_3 \right]; \quad i = 1,2 \tag{A.6}$$

$$S_{i2}^{(1)}(r) = T_{i2}^{(1)}(K_{T1}r) + \frac{1}{\delta}\left[\bar{T}_{i1}^{(1)}(K_{L1}r)X_2 + \bar{T}_{i2}^{(1)}(K_{T1}r)X_4 \right]; \quad i = 1,2 \tag{A.7}$$

REFERENCES

1. Abramowitz, M. and Stegun, I.A. (1965). “Handbook of Mathematical Functions”, Dover, New York, U.S.A.
2. Coussy, O. (1984). “Scattering of Elastic Waves by an Inclusion with an Interface Crack”, Wave Motion, Vol. 6, No. 2, pp. 223-236.
3. Coussy, O. (1986). “Scattering of SH-Waves by a Rigid Elliptic Cylinder Partially Debonded from its Surrounding Matrix”, Mechanics Research Communications, Vol. 13, No. 1, pp. 39-45.
4. Dundurs, J. (1969). “Discussion: Edge-Bonded Dissimilar Orthogonal Elastic Wedges under Normal and Shear Loading by D.B. Bogy”, Journal of Applied Mechanics, ASME, Vol. 36, pp. 650-652.
5. Mal, A.K., Ang, D.D. and Knopoff, L. (1968). “Diffraction of Elastic Waves by a Rigid Circular Disc”, Proceedings of the Cambridge Philosophical Society, Vol. 64, pp. 237-247.
6. Manolis, G.D. and Beskos, D.E. (1988). “Boundary Element Methods in Elastodynamics”, Unwin Hyman, London, U.K.
7. Pao, Y.H. and Mow, C.C. (1973). “Diffraction of Elastic Waves and Dynamic Stress Concentrations”, Crane Russak, New York, U.S.A.

8. Sato, H. and Shindo, Y. (2002). "Influence of Microstructure on Scattering of Plane Elastic Waves by a Distribution of Partially Debonded Elliptical Inclusions", Mechanics of Materials, Vol. 34, No. 7, pp. 401-409.
9. Wang, X.D. and Meguid, S.A. (1999). "Dynamic Interaction between a Matrix Crack and a Circular Inhomogeneity with a Distinct Interphase", International Journal of Solids and Structures, Vol. 36, No. 4, pp. 517-531.
10. Wang, Y.S. and Wang, D. (1994a). "Diffraction of SH Waves by a Circular Cavity with a Partially Debonded Liner", Acta Mechanica Sinica, Vol. 26, No. 4, pp. 462-469 (in Chinese).
11. Wang, Y.S. and Wang, D. (1994b). "Elastic Wave Scattering from a Partially Debonded Elastic Cylindrical Inclusion", Journal of Harbin Institute of Technology, Vol. E1, No. 1, pp. 71-79.
12. Wang, Y.S. and Wang, D. (1996). "Scattering of Elastic Waves by a Rigid Cylindrical Inclusion Partially Debonded from its Surrounding Matrix ─ II. P and SV Cases", International Journal of Solids and Structures, Vol. 33, No. 19, pp. 2817-2840.
13. Yang, Y. and Norris, A. (1992). "Longitudinal Wave Scattering from a Partially Bonded Fiber", Wave Motion, Vol. 15, No. 1, pp. 43-59.
14. Zhang, Ch. and Gross, D. (1998). "On Wave Propagation in Elastic Solids with Cracks", Computational Mechanics, Southampton, U.K.